

Numerical Analysis of Transient Responses for Elastic Structures Connected to a Viscoelastic Shock Absorber Using FEM with a Nonlinear Complex Spring

Takao Yamaguchi¹, Yusaku Fujii, Toru Fukushima², Akihiro Takita¹, Suguru Ota²,
Norihisa Tomita and Tatsuya Noto

¹ Gunma University
Tenjin-cho 1-5-1, Kiryu, Gunma, Japan
² Graduate School of Gunma University
Tenjin-cho 1-5-1, Kiryu, Gunma, Japan
yamagme3@gunma-u.ac.jp

Abstract

This paper describes numerical simulation of impact responses for a viscoelastic shock absorber connected with a S-shaped structure using a finite element method. This S-shaped structure is a part of a force transducer. And the shock absorber is a specimen to be measured its impact responses when the levitated mass is collided with it. In this analysis, the viscoelastic absorber is modelled by using a nonlinear complex spring to describe its nonlinear hysteresis under relatively large deformation. One end of this nonlinear spring is connected to the S-shaped structure. The other end is connected to the levitated block. The S-shaped structure and the block are modelled by three-dimension finite elements. The levitated block has initial velocities and collides with the shock absorber. Acceleration of the S-shaped elastic structure and the levitated block are measured using Levitation Mass Method proposed by Fujii. The calculated accelerations from the proposed FEM, corresponds to the experimental ones. Moreover, using this method, we also investigate dynamic errors of the S-shaped force transducer due to elastic modes in the S-shaped structure.

1 Introduction

Various viscoelastic shock absorbers are utilized to diminish impacts from precision instruments and so on. Under relatively large deformation, the viscoelastic absorbers sometimes have nonlinearity between their restoring forces and deformations [8-10]. Moreover, their restoring forces sometimes have nonlinearity in hysteresis. Therefore, it is important to investigate nonlinear dynamic characteristics of viscoelastic absorbers connected to elastic structures under impact load.

Using a fast finite element method proposed by Yamaguchi [1-2], this paper describes numerical simulation of impact responses for a viscoelastic shock absorber connected with an elastic structure. As an example of the elastic structure, we deal with an S-shaped structure, which is a part of a force transducer as shown in Fig.1. In this simulation, the viscoelastic absorber is modeled by using a nonlinear complex spring. The restoring force of the spring is expressed as power series of its relative displacement between two ends. The restoring force also involves nonlinear hysteresis damping because the hysteresis depends on its deformation. We introduce complex spring constants for not only the linear component but also nonlinear components of the restoring force. We express a finite element of the nonlinear complex spring and the spring is connected to an S-shaped elastic structure modeled by linear finite elements.

The discretized equations of these structures are transformed from physical coordinate to the nonlinear ordinary coupled equations using normal coordinate corresponding to linear eigenmodes. Further, we integrate the transformed equations numerically in drastically small degree-of-freedom.

In this paper, our proposed FEM is applied to clarify dynamic errors in the S-shaped force transducer when we measure transient responses of the viscoelastic shock absorber. The transient responses are obtained when the levitated block is collided with the absorber. We check the validity of the calculated results in comparison with the experimental results.

Further, to evaluate the dynamic errors in the force transducer, the reference force is also measured using Levitation Mass Method proposed by Fujii [3]. We checked dynamic errors between the reference force and the force measured by the transducer itself in the previous paper [3]. The experimental dynamic errors [3] are compared with the calculated data from our proposed FEM. Moreover, we investigate and find out the causes of the dynamic errors as nonlinear oscillation phenomena.

2 Experimental setup and results [3]

Figure 1 shows a schematic diagram of the experimental setup performed by Fujii in the previous paper [3]. An S-shaped force transducer, shown in the photograph in Fig.2, is connected with a viscoelastic shock absorber. To evaluate impact responses of the viscoelastic absorber, a block levitated by linear pneumatic bearing is collided with the absorber in z direction. And their transient responses are measured using the force transducer. As shown in Fig.2, the S-shaped structure in the force transducer contains two thin

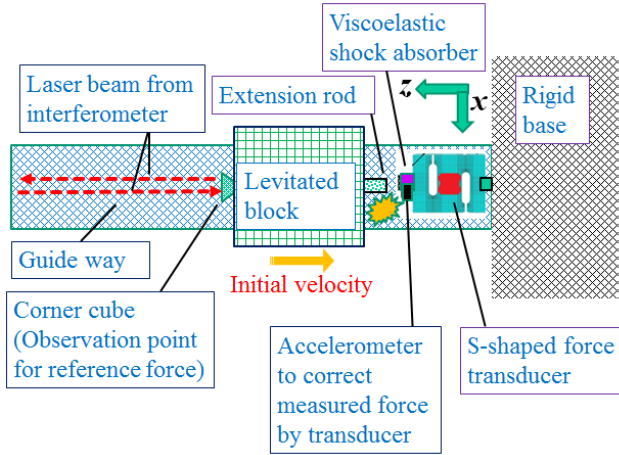


Figure 1: Outline of experimental system [3]

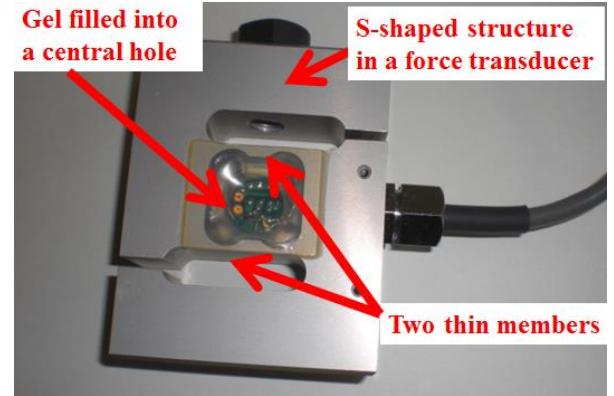


Figure 2: Photograph of the S-shaped force transducer [3]

members in the vicinity of a central hole. These two members correspond to a pair of parallel springs in z direction. Strains are measured using strain gauges attached in the S-shaped structure when external dynamic load is exerted in z direction. Using a bridge circuit and the measured strains, forces F_{trans} of the impact responses are measured.

To validate accuracy of the measured force F_{trans} , Fujii additionally measured the velocity v_1 of the levitated block using an interferometer as illustrated in Fig.1. Firstly, acceleration a_1 of the levitated block can be identified by differentiating the measured velocity v_1 with respect to time. The reference force $F_{mass} = M_1 a_1$ is obtained using the acceleration a_1 and mass $M_1 = 2.6526\text{kg}$ of the levitated block if the block can be regarded as a concentrated mass. In the previous paper [3], Fujii compared between the reference force F_{mass} and the force F_{trans} measured from the S-shaped transducer itself as shown in Fig.3. And he found out that

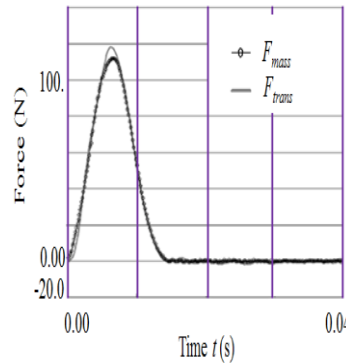


Figure 3: Comparison between the measured force F_{trans} the S-shaped transducer and the reference force F_{trans} using Levitation Mass Method [3]

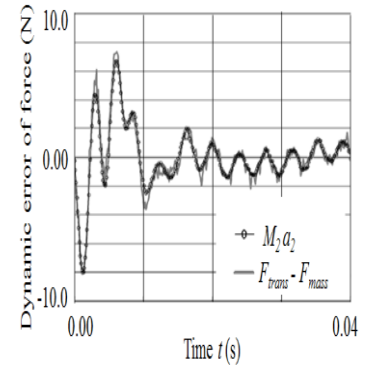


Figure 4: Comparison between the measured dynamic error $\Delta F = F_{trans} - F_{mass}$ and the estimated error using acceleration $M_2 a_2$ of the S-shaped structure [3]

small dynamic errors are hidden in the measured force F_{trans} of the S-shaped transducer. In Fig.4, a time history of the difference $\Delta F = F_{trans} - F_{mass}$ between the measured force F_{trans} by the transducer itself and the reference force F_{mass} . Fujii pointed out that the difference $\Delta F = F_{trans} - F_{mass}$ are related with $M_2 a_2$. a_2 is the acceleration of the S-shaped structure and M_2 is mass of a half portion of the S-shaped structure. Fujii proposed a correction of the measured force F_{trans} by the transducer itself using an expression $\Delta F \cong M_2 a_2$. To estimate correction force ΔF , Fujii fabricated an accelerometer to the movable half portion in the S-shaped

structure as illustrated in Fig.1. The measured acceleration a_2 from the accelerometer is used to correct the measured force F_{trans} in real time. In this paper, numerical analysis for this experimental system are carried out to investigate the correction force ΔF which corresponds to the difference between F_{trans} and F_{mass} .

These experimental data are compared with our computed data in this paper to validate our proposed FEM with consideration of nonlinear complex springs.

To get the reference force F_{mass} , Levitation Mass Method (i.e. LMM) is utilized. The detail setup and procedure of the LMM experimental system are noted as follows. As illustrated in Fig.1, the LMM experimental system contains a levitated mass (i.e. this corresponds to a levitated rigid block), which is able to move along a guide way in z direction due to a pneumatic linear bearing. The block is levitated due to air film at the interfaces between the block and the guide. Thickness of the air film is $8 \mu\text{m}$. Pressure at the interfaces is self-controlled by orifice effect to keep the thickness of the air film. Due to this system, the block can travel in the z -direction with extremely low friction. An extension rod is fabricated on the levitated mass. Initial velocities v_0 are given with the levitated block manually. The block is collided with the viscoelastic shock absorber connected with the S-shaped force transducer. This sophisticated experimental system is named as Levitation Mass method by Fujii [4-6]. Near the transducer, the accelerometer is fabricated as we mentioned before. One end of the S-shaped force transducer is fixed on the rigid base. Note that a gel is filled in the central hole of the S-shaped structure to increase damping as shown in Fig.2.

3 Numerical simulation

As shown in Fig.5, we evaluate the FEM model for the S-shaped structure in the force transducer. Both the S-shaped structure and the levitated block are modeled as an elastic body using three dimensional finite elements. The viscoelastic shock absorber is modelled by a nonlinear spring with nonlinear damping using nonlinear complex spring constants. We set the origin of this model on the position where the levitated block begins to contact with the viscoelastic shock absorber. We give an initial velocity $v_0 = -180$ (mm/sec) in z -direction to the levitated block by a hand.

3.1 Discretized equation for the viscoelastic absorber

Using a concentrated nonlinear spring with nonlinear hysteresis, the viscoelastic absorber is expressed. To express the nonlinear hysteresis, we propose and introduce a nonlinear complex spring. We set that the nonlinear complex spring with viscoelasticity has principal elastic axis in z direction as shown in Fig.5. We denote the displacement in z direction at the nodal point α as $U_{\alpha z}$ where the S-shaped force transducer is attached with one end of the nonlinear complex spring (i.e. the viscoelastic absorber). $U_{\beta z}$ is the displacement at the nodal point β on another end of the nonlinear complex spring. At this nodal point β , the levitated block is connected with the viscoelastic absorber. We use nonlinear function using power series for the nodal force of the complex spring at the point α . Thus, the restoring force of the complex spring is expressed using the relative displacement $U_{\alpha z} - U_{\beta z}$ between $U_{\alpha z}$ and $U_{\beta z}$ as follows.

$$R_{\alpha z} = \gamma_1(U_{\alpha z} - U_{\beta z}) + \gamma_2(U_{\alpha z} - U_{\beta z})^2 + \gamma_3(U_{\alpha z} - U_{\beta z})^3 \quad (1)$$

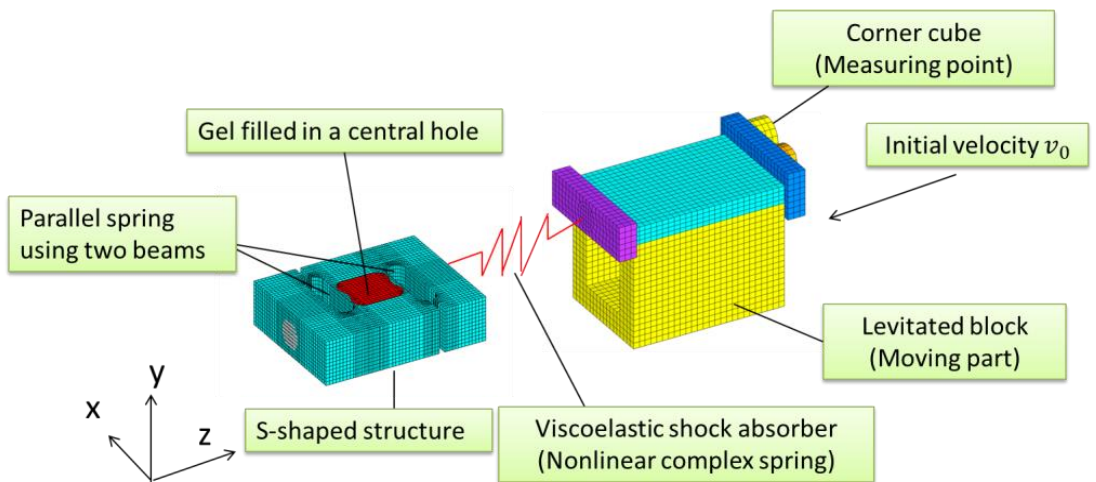


Figure 5: Simulation model

Firstly, we introduce conventional linear hysteresis damping as $\gamma_1 = \bar{\gamma}_1(1 + j\eta_{s1})$. j is imaginary unit. $\bar{\gamma}_1$ is the real part of γ_1 and η_{s1} is material loss factor of the concentrated spring. Further, we propose and introduce nonlinear hysteresis damping as $\gamma_2 = \bar{\gamma}_2(1 + j\eta_{s2})$ and $\gamma_3 = \bar{\gamma}_3(1 + j\eta_{s3})$ in the same manner. $\bar{\gamma}_2$ and $\bar{\gamma}_3$ are the real part of γ_2 and γ_3 , respectively. η_{s2} and η_{s3} are nonlinear components of material loss factor for the concentrated spring, respectively. For the nonlinear complex spring, nonlinear spring constants have complex quantity to represent changes of hysteresis due to the deformation of the spring. The restoring force of the nonlinear complex spring can be written in the matrix form as follows.

$$R_{\alpha} = \{r\} = [\gamma_1]\{U_s\} + \{\bar{d}\} \quad (2)$$

$$\{r\} = \begin{Bmatrix} 0 \\ 0 \\ R_{\alpha\alpha} \\ 0 \\ 0 \\ R_{\beta\beta} \end{Bmatrix}, \{U_s\} = \begin{Bmatrix} U_{\alpha x} \\ U_{\alpha y} \\ U_{\alpha z} \\ U_{\beta x} \\ U_{\beta y} \\ U_{\beta z} \end{Bmatrix}, [\gamma_1] = \begin{bmatrix} 0 & 0 & 0 & 0 & 0 & 0 \\ 0 & 0 & 0 & 0 & 0 & 0 \\ 0 & 0 & \gamma_1 & 0 & 0 & -\gamma_1 \\ 0 & 0 & 0 & 0 & 0 & 0 \\ 0 & 0 & 0 & 0 & 0 & 0 \\ 0 & 0 & -\gamma_1 & 0 & 0 & \gamma_1 \end{bmatrix}, \{\bar{d}\} = \begin{Bmatrix} 0 \\ 0 \\ +\gamma_2(U_{\alpha x} - U_{\beta x})^2 + \gamma_3(U_{\alpha x} - U_{\beta x})^3 \\ 0 \\ 0 \\ -\gamma_2(U_{\alpha x} - U_{\beta x})^2 - \gamma_3(U_{\alpha x} - U_{\beta x})^3 \end{Bmatrix}$$

Where $\{U_s\}$ is the nodal displacement vector at the nodes. $\{r\}$ is the nodal force vector at the nodes α and β . $\{\bar{d}\}$ is the vector including nonlinear terms of the restoring force. $[\gamma_1]$ is the complex stiffness matrix containing only linear term of the restoring force. The following linear and nonlinear complex spring constants are used for the later computations.

$$\bar{\gamma}_1 = 1.37 \times 10^4 \text{ (N/m)}, \bar{\gamma}_2 = 0.00 \text{ (N/m}^2\text{)}, \bar{\gamma}_3 = 2.35 \times 10^{11} \text{ (N/m}^3\text{)}, \eta_{s1} = 0.300, \eta_{s2} = 0.000, \eta_{s3} = 0.300.$$

3.2 Discretized equations of the S-shaped force transducer and the levitated block

For the elastic structure of the S-shaped force transducer and the levitated block, we assumed that equations of motion are expressed under infinitesimal deformation using conventional three-dimensional finite elements. These are made by aluminium. To add damping effects, a viscoelastic gel is filled in the central hole of the force transducer as shown in Fig.2. Thus, we also create the three dimensional finite elements for the gel as depicted in Fig.5. Viscoelasticity of the gel is taken into account using complex modulus of elasticity $\bar{E}_g = E_g(1 + j\eta_g)$. The real part E_g of the \bar{E}_g stands for the storage modulus of elasticity while η_g is the material loss factor of the gel. By superposing all elements related to the S-shaped transducer, the levitated block and the gel, the following equations are obtained.

$$[M_s]\{\ddot{u}_s\} + [K_s]\{u_s\} = \{f_s\} \quad (3)$$

$$[M_g]\{\ddot{u}_g\} + [K_g]\{u_g\} = \{f_g\} \quad (4)$$

$$[M_L]\{\ddot{u}_L\} + [K_L]\{u_L\} = \{f_L\} \quad (5)$$

Where, $[M_s]$, $[K_s]$, $\{f_s\}$ and $\{u_s\}$ are the mass matrix, complex stiffness matrix, nodal force vector and displacement vector for the elements of the S-shaped transducer denoting by the subscripts s in Eq. (3). The subscripts g in Eq. (4) and subscripts L in Eq. (5) denote the gel and the levitated block, respectively. For the three dimensional finite elements of these solid structures, isoparametric hexahedral elements with non-conforming modes [11-12] are mainly adopted.

3.3 Discrete equation for combined system among the S-shaped force transducer, the viscoelastic absorber and the levitated block

In Eq. (2), the restoring force $\{r\}$ is added to the nodal force at the ends of the nonlinear complex spring on the nodes α and β . On the node α , the nonlinear complex spring (i.e. the viscoelastic shock absorber) is

connected with the S-shaped force transducer in Eq.(3). On the node β , the spring is also connected with the levitated block in Eq.(5). Finally, the following expression in global system can be obtained using Eqs.(2)-(5).

$$[M]\{\ddot{u}\} + [K]\{u\} + \{\hat{d}\} = \{f\} \quad (6)$$

Where, $\{f\}$, $[M]$, $[K]$ and $\{u\}$ are the displacement vector, mass matrix, complex stiffness matrix and external force vector in global system, respectively. $\{\hat{d}\}$ is modified from $\{\bar{d}\}$ to have the identical vector size to degree-of-freedom of the global system.

3.4 Approximate calculation of modal damping

Under infinitesimal deformation, we use the following complex eigenvalue problem of Eq. (6) by neglecting the terms of the nonlinear restoring force and the external force to calculate modal loss factors as imaginary part of eigenvalues. These parameters correspond to linear modal damping.

$$\sum_{e=1}^{e_{\max}} (-\omega^{(i)})^2 (1 + j\eta_{tot}^{(i)}) [M]_e + [K_R]_e (1 + j\eta_e) \{\phi^{(i)}\} = \{0\} \quad (7)$$

where, $(\omega^{(i)})^2$ is the real part of complex eigenvalue. $\{\phi^{(i)}\}$ is the complex eigenvector and $\eta_{tot}^{(i)}$ is the modal loss factor. η_e contains η_{s1} and η_g . Superscript (i) denotes the i -th eigenmode. Next, the following β_e are introduced using the maximum value η_{\max} among the elements' material loss factors η_e , ($e = 1, 2, 3, \dots, e_{\max}$).

$$\beta_e = \eta_e / \eta_{\max}, \beta_e \leq 1 \quad (8)$$

Solutions of Eq.(7) are expanded using a small parameter $\mu = j\eta_{\max}$ on assumption of $\eta_{\max} \ll 1$ as follows [13],[2].

$$\{\phi^{(i)}\} = \{\phi^{(i)}\}_0 + \mu\{\phi^{(i)}\}_1 + \mu^2\{\phi^{(i)}\}_2 + \dots \quad (9)$$

$$(\omega^{(i)})^2 = (\omega_0^{(i)})^2 + \mu^2(\omega_2^{(i)})^2 + \mu^4(\omega_4^{(i)})^2 + \dots \quad (10)$$

$$j\eta_{tot}^{(i)} = \mu\eta_1^{(i)} + \mu^3\eta_3^{(i)} + \mu^5\eta_5^{(i)} + \mu^7\eta_7^{(i)} + \dots \quad (11)$$

Above equations, we can obtain $\eta_{\max}\beta_e \ll 1$ under conditions of $\beta_e \leq 1$ and $\eta_{\max} \ll 1$. Therefore, $\mu\beta_e$ also become small parameter like μ .

In the equations, $(\omega_0^{(i)})^2$, $(\omega_2^{(i)})^2$, $(\omega_4^{(i)})^2$, ... and $\eta_1^{(i)}$, $\eta_3^{(i)}$, $\eta_5^{(i)}$, ... have real quantities. By Substitution of Eqs.(9)-(11) into Eq. (7), we obtain approximate equations using μ^0 and μ^1 orders. As a result, the following equation can be derived by arranging the approximate equations [13],[2].

$$S_e^{(i)} = \{\phi^{(i)}\}_0^T [K_R]_e \{\phi^{(i)}\}_0 / \sum_{e=1}^{e_{\max}} (\{\phi^{(i)}\}_0^T [K_R]_e \{\phi^{(i)}\}_0) \quad (12)$$

From these expressions, we can calculate modal loss factor $\eta_{tot}^{(i)}$ using material loss factors η_e of each element e , share $S_e^{(i)}$ of strain energy of each element to total strain energy.

3.5 Conversion from the discretized equation in physical coordinate to the nonlinear equation in normal coordinate

If we compute Eq.(6) directly in physical coordinate, it requires much computational time because of large degree-of-freedom. Therefore, we introduce computational method to diminish the degree-of-freedom for the discretized equations of motion Eq.(6).

It is assumed that we approximate linear natural modes $\{\phi^{(i)}\}$ of vibration to $\{\phi^{(i)}\}_0$. The nodal displacement vector $\{u\}$ can be expressed using both $\{\phi^{(i)}\}_0$ and \tilde{b}_i by introducing normal coordinates \tilde{b}_i corresponding to the linear natural modes $\{\phi^{(i)}\}_0$ [14].

$$\{u\} = \sum_i \tilde{b}_i \{\phi^{(i)}\}_0 \quad (13)$$

By substitution of Eq.(13) into Eq.(6), we obtain the following nonlinear ordinary simultaneous equations as to normal coordinates \tilde{b}_i .

$$\begin{aligned} \tilde{b}_{i,t} + \eta_{tot}^{(i)} \omega_0^{(i)} \tilde{b}_{i,t} + (\omega_0^{(i)})^2 \tilde{b}_i + \sum_j \sum_k \tilde{D}_{ijk} \tilde{b}_j \tilde{b}_k + \sum_j \sum_k \sum_l \tilde{E}_{ijkl} \tilde{b}_j \tilde{b}_k \tilde{b}_l = \tilde{P}_i, (i, j, k, l = 1, 2, 3, \dots) \quad (14) \\ \tilde{P}_i = \{\phi^{(i)}\}_0^T \{f\}, \{\phi^{(i)}\}_0 = \{\phi_{1ix}, \phi_{1iy}, \phi_{1iz}, \phi_{2ix}, \phi_{2iy}, \phi_{2iz}, \phi_{3ix}, \dots\}^T, \tilde{D}_{ijk} = \gamma_2 (\phi_{\alpha iz} - \phi_{\beta iz}) (\phi_{\alpha jz} - \phi_{\beta jz}) (\phi_{\alpha kz} - \phi_{\beta kz}), \\ \tilde{E}_{ijkl} = \gamma_3 (\phi_{\alpha iz} - \phi_{\beta iz}) (\phi_{\alpha jz} - \phi_{\beta jz}) (\phi_{\alpha kz} - \phi_{\beta kz}) (\phi_{\alpha lz} - \phi_{\beta lz}) \end{aligned}$$

where, $\eta_{tot}^{(i)}$ is the i -th modal loss factor. $\omega_0^{(i)}$ represents the i -th eigenfrequency. Subscript t following a comma denotes partial differentiation with respect to time t . $\phi_{\alpha iz}$ is the z -component of the eigenmode $\{\phi^{(i)}\}_0$ at the connected node α between the S-shaped force transducer and the viscoelastic shock absorber. We can save computational time drastically because Eq. (14) has much smaller degree-of-freedom than that of Eq.(6).

3.6 Nonlinear impact response

An initial velocity is given to the levitated block attached with the viscoelastic shock absorber. And nonlinear impact responses of the viscoelastic absorber with the S-shaped structure are computed by applying Runge-Kutta-Gill method to Eq.(14).

4 Numerical results and discussion

4.1 Validity of the proposed FEM

In this section, we validate our proposed finite element method in consideration of nonlinear hysteresis

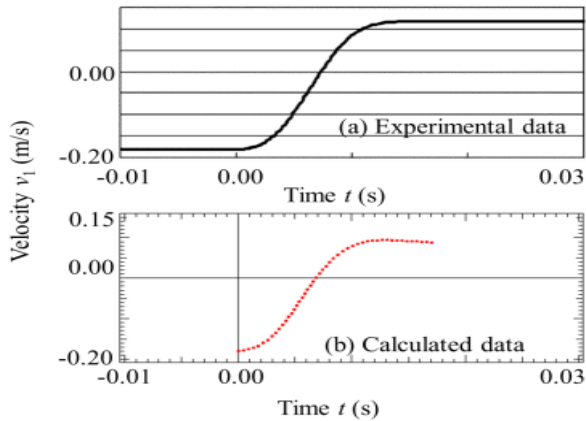


Figure 6: Comparison of the velocity between calculated and experimental data [3]

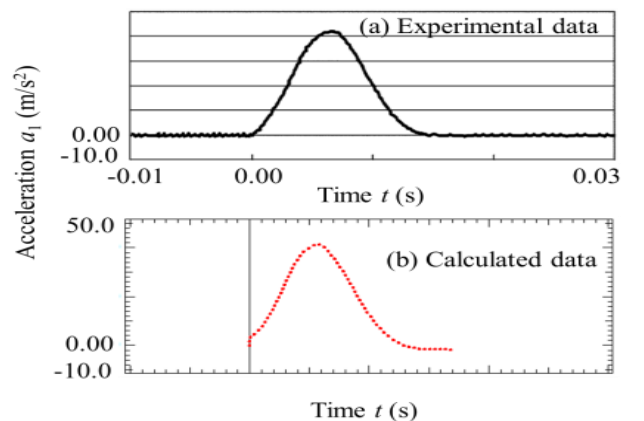


Figure 7: Comparison of the acceleration between calculated and experimental data [3]

using nonlinear complex springs.

First, we check the calculated results of the reference forces. Fig.6 shows time histories of the measured and calculated velocities v_1 at the corner cube on the levitated block. In Fig.7, the experimental and calculated accelerations a_1 at the corner cube are compared. Further, the experimental and calculated reference forces F_{mass} using a_1 of the levitated block are shown in Fig.8. In these graphs, we set the origin of time when the levitated block starts to contact with the viscoelastic shock absorber connected with the S-shaped structure. From these graphs in Figs.6-8, the calculated time histories agree well with the experimental ones for the velocities v_1 , accelerations a_1 and the reference force F_{mass} . Therefore, the validity of our proposed FEM is confirmed to compute the reference force in the impact response of the viscoelastic shock absorber.

Further, we compute and investigate dynamic errors of the S-shaped force transducer. Fujii point out in the previous paper [3] that there exists a relation of $\Delta F \cong M_2 a_2$ for the dynamic errors ΔF in the measured force of the transducer. a_2 is the

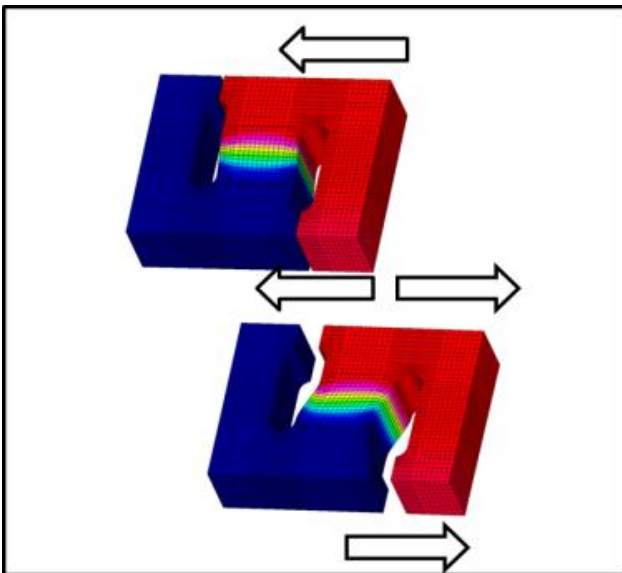


Figure 10: Elastic mode of the S-shaped structure in z-direction

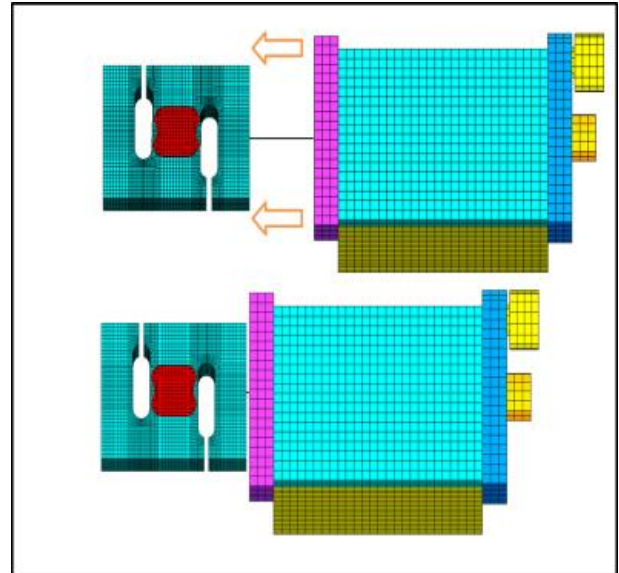


Figure 11: Elastic mode of the nonlinear complex spring in z-direction

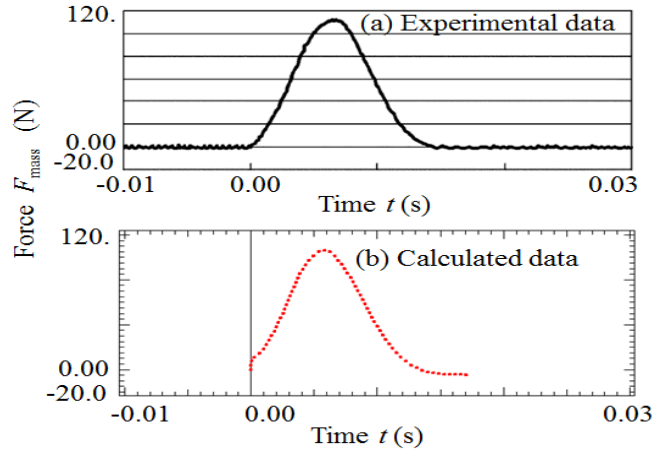


Figure 8: Comparison of the reference force between calculated and experimental data [3]

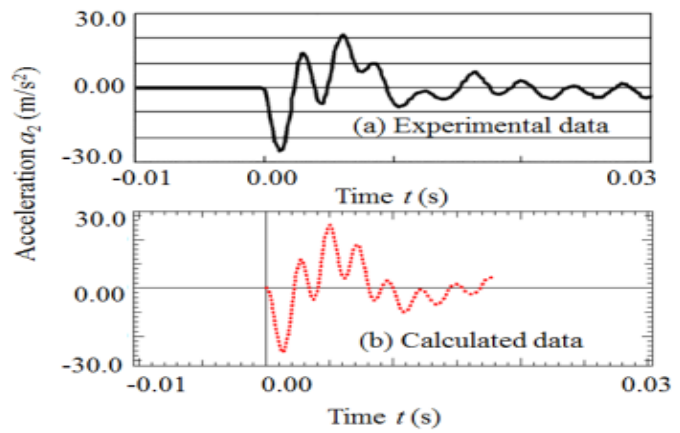


Figure 9: Comparison of the accelerations at the S-shaped structure between calculated and experimental data [3]

signal of the acceleration from the accelerometer fixed on the S-shaped structure, while M_2 is the half of the mass for the S-shaped structure in the transducer. From this viewpoint, we also compute the acceleration a_2 on the S-shaped structure in the transducer to clarify the dynamic errors. As shown in Fig.9 (a), the experimental acceleration a_2 of the S-shaped structure in the transducer is much different qualitatively from the acceleration a at the levitated block shown in the Fig.7 (a). There exist high frequency components in the waveform of the acceleration a_2 in the transducer.

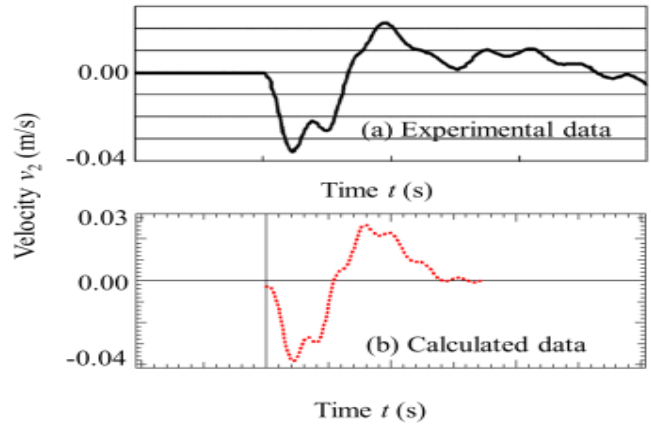


Figure 12: Comparison of the velocities at the S-shaped structure between calculated and experimental data [3]

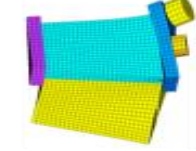
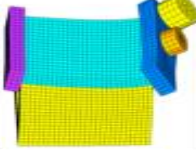
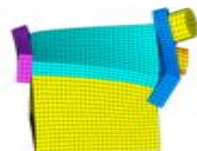
| | | | |
|-------------------|---|--|---|
| modal |  |  |  |
| Frequency (Hz) | 0.632×10^4 | 0.751×10^4 | 0.898×10^4 |
| Modal loss factor | 0.508×10^{-4} | 0.504×10^{-4} | 0.503×10^{-4} |

Figure 13: Resonant frequencies and Modal loss factors of elastic modes of the levitated block

Therefore, to clarify dynamic errors of the force transducer, we try to investigate what happens in this system. The corresponding calculated time history of the acceleration a_2 in the transducer is shown in Fig.9 (b). In comparison with the experimental data in Fig.9 (a), both time histories agree well. We can confirm that our proposed FEM in consideration of nonlinear complex springs is valid. We can recognize that there are typical periods in the accelerations a_2 at the S-shaped structure in the force transducer. We can find a short period 0.0025(S) in the waveform. This corresponds to the eigen frequency of the elastic mode for the S-shaped structure of the transducer in z -direction. The deformation in this eigenmode is shown in Fig.10. From this figure, the half portion of the S-shaped structure deforms. Another half portion never moves. This implies that the dynamic motion of the half portion for the S-shaped structure is dominant. We can regard that the correction force $\Delta F \cong M_2 a_2$ using the half mass M_2 of the S-shaped structure is reasonable. In Fig.9, a long period 0.013 (s) is also found. We can find out an internal resonance due to the nonlinearity of the viscoelastic shock absorber in this period. This long period has a relation with the superharmonic component of order seven for the rigid translation of the levitated block in the z -direction as shown in Fig.11. Moreover,

this is related with the subharmonic component of order 1/7 for the elastic mode of the S-shaped structure in Fig.10.

We also check velocities at the S-shaped structure in Fig.12. The calculated velocity is consistent with the experimental one.

4.2 Numerical analysis to confirm accuracy of the reference force using LMM

In this section, by evaluating measurement errors due to undesirable motions or deformation of the levitated block, we check the accuracy [7] of the reference force using the Levitation Mass Method. Elastic eigenmodes of the levitated block are shown in Fig.13. If these modes are generated when the levitated block is collided with the viscoelastic shock absorber with the S-shaped force transducer, measurement errors of the reference force increase. To check these errors, we consider the consistency between the displacement D_g at the center of gravity of the levitated block and the displacement D_c at the corner cube. As a result, the ratio $D_c / D_g = 0.9997417311 \cong 1.00$ is obtained at $t=0.00704$ [sec]. Note that the displacements reach the local maximal value at $t=0.00704$ [sec]. From this ratio, the undesirable dynamic motions and deformations of the levitated block can be regarded as enough small. Thus, the reference force as shown in Fig.8 includes enough small measurement errors due to the undesirable behaviours of the levitated block.

5 Conclusion

This paper deals with numerical analysis of impact responses for a viscoelastic shock absorber connected with an elastic structure (an S-shaped structure) using a fast finite element method proposed by Yamaguchi. In this analysis, the viscoelastic absorber is modelled by using a nonlinear complex spring. The restoring force of the spring is expressed as power series of its elongation (e.g. relative displacement between the ends of the complex nonlinear spring). The restoring force also includes nonlinear hysteresis damping. Therefore, complex spring constants are introduced for not only the linear component but also nonlinear components of the restoring force. Finite element for the nonlinear complex spring is expressed and is connected to an elastic structure modelled by linear solid finite elements. The discrete equations of this system in physical coordinate are transformed into the nonlinear ordinary coupled equations using normal coordinate corresponding to linear natural modes. The transformed equations are integrated numerically in extremely small degree-of-freedom. In this paper, we apply our proposed FEM to examine dynamic errors in an S-shaped force transducer when transient responses of a viscoelastic shock absorber are measured. The transient responses are obtained when a levitated block is collided with the absorber. The elastic structures in this study are the levitated block and the S-shaped structure, which is a part of the force transducer. These are expressed by using linear solid finite elements. The viscoelastic shock absorber is modelled by using the complex nonlinear spring. The nonlinear complex spring is attached between the levitated block and the s-shaped structure. To check the dynamic errors in the transducer, the reference force is also measured using Levitation Mass Method proposed by Fujii. In this method, the block is levitated by a pneumatic bearing. A corner cube is fabricated on the block to receive a laser beam from an interferometer. The velocity of the levitated block is measured using the interferometer. The experimental dynamic errors are well simulated with the calculated ones from our proposed FEM. We find out that the dynamic errors are due to nonlinear dynamic responses of the eigenmode of the S-shaped structure.

Acknowledgments

This work was supported by JSPS KAKENHI Grant Number 24360156.

References

- [1] T. Yamaguchi, Y. Fujii, T. Fukushima, N. Tomita, A. Takita, K. Nagai and S. Maruyama, *Damping response analysis for a structure connected with a nonlinear complex spring and application for a finger protected by absorbers under impact forces*, Mechanical Systems and Signal Processing, (in press).

- [2] T. Yamaguchi, Y. Fujii, K. Nagai and S. Maruyama, *FEM for vibrated structures with non-linear concentrated spring having hysteresis*, Mechanical Systems and Signal Processing, , Vol. 20 (2006), pp. 1905-1922.
- [3] Y. Fujii, *Measurement of the electrical and mechanical responses of a force transducer against impact forces*, Review of Scientific Instruments, Vol. 77, Aug. (2006), pp. 1-5.
- [4] Y. Fujii and T. Yamaguchi, *Impact response measurement of a human arm*, Experimental Techniques, , May/June (2006), pp. 64-68.
- [5] Y. Fujii and T. Yamaguchi, *Method for evaluating material viscoelasticity*, Review of Scientific Instruments, Vol. 75, No.1 (2004), pp. 119-123.
- [6] Y. Fujii and T. Yamaguchi, *Proposal for material viscoelasticity evaluation method under impact load*, Journal of Material Science, Vol. 40, No.18 (2005), pp. 4785-4790.
- [7] T. Yamaguchi, Y. Fujii, K. Nagai and S. Maruyama, *Dynamic analysis by FEM for a measurement system to observe viscoelasticity using levitation mass method*, International Journal of Advanced Manufacturing and Technology, Vol. 46, No.9-12 (2010), pp. 885-891.
- [8] B. F. Feeny and R. Kappagantu, *On the physical interpretation of proper orthogonal modes in vibrations*, Journal of Sound and Vibration, Vol. 211, No.4 (1998), pp. 607-616.
- [9] T. Kondo, T. Sasaki and T. Ayabe, *Forced vibration analysis of a straight-line beam structure with nonlinear support elements*, Transactions of the Japan Society of Mechanical Engineers, Vol. 67, No.656C (2001), pp. 914-921.
- [10] E. Pesheck, N. Boivin, C. Pierre and S. W. Shaw, *Non-linear modal analysis of structural systems using multi-mode invariant manifolds*, Nonlinear Dynamics, Vol. 25 (2001), pp. 914-921.
- [11] O. C. Zienkiewicz and Y. K. Cheung, *The finite element method in structural and continuum mechanics*, MacGraw-Hill (1967).
- [12] E. L. Wilson, R. L. Taylor, W. P. Doherty and J. Ghaboussi, *Incompatible displacement methods, in numerical and computer methods in structural mechanics*, Academic Press (1973).
- [13] B. A. Ma and J. F. He, *A finite element analysis of viscoelastically damped sandwich plate*, Journal of Sound and Vibration, Vol. 152, No.1 (1992), pp. 107-123.
- [14] T. Yamaguchi and K. Nagai, *Chaotic vibration of a cylindrical shell-panel with an in-plane elastic support at boundary*, Nonlinear Dynamics, Vol. 13 (1997), pp. 259-277.